Trapped-Electron Mode in Cylindrical Geometry*

C. A. Primmerman, L. M. Lidsky, and P. A. Politzer
Department of Nuclear Engineering and Research Laboratory of Electronics, Massachusetts Institute of Technology, Cambridge, Massachusetts 02139
(Received 11 July 1974)

The theory of the cylindrical-geometry analog to the toroidal trapped-electron-scattering mode has been developed, and the resulting equations have been solved numerically. Observations of oscillations occurring near the electron bounce frequency have been made in a plasma confined by a spatially periodic magnetic field. These oscillations were found to be low-amplitude, high-mode-number, drift-type modes having properties consistent with theoretical predictions.

Recent interest in tokamaks with reactor parameters has resulted in considerable speculation concerning the possible deleterious effects of trapped particles. A product of this speculation has been the prediction of no less than fifteen distinct trapped-particle modes,[1,2] many of which are presumed to have important consequences for particle transport and thermal energy transfer. Unfortunately, verification of these modes has been lacking, since tokamaks have yet to reach banana-orbit regimes. In linear machines, contradistinctively, trapped-particle modes are of little practical importance, but plasmas sufficiently collisionless to operate in a trapped-particle regime are easily produced. Linear machines offer a number of other significant advantages over tokamaks: They may be run in a steady-state mode; the trapping-well depth, rather than being fixed by geometry, is a free parameter; probes may be used to measure spatial profiles accurately. Thus, while trapped-particle modes are of greater significance for toroidal devices, these modes may be more easily investigated and identified in cylindrical devices.

In this Letter we outline the development of the cylindrical-geometry analog to the toroidal trapped-electron-scattering mode first predicted by Coppi,[3] and investigated by Coppi and Rewoldt.[2] We list the basic theoretical predictions for this mode and compare them to the properties of modes we have observed in a linear machine with spatially periodic magnetic field.

We take as a model an infinite, cylindrical plasma confined by a periodic magnetic field with variation given by

$$\vec{B}=\hat{k}B_z=\hat{k}B_0[1-\epsilon\cos(2\pi z/L)], \tag{1}$$

where ϵ is a small number, and L is the distance between mirrors. We consider the low-β limit and look for electrostatic oscillations of the form

$$\tilde{\Phi}=\tilde{\varphi}_m(z)\exp(im\theta-i\omega t), \tag{2}$$

where $\tilde{\varphi}_m(z)$ is a periodic function in z depending on L, the magnetic field period. In particular, we will specialize to $\tilde{\varphi}_m(z)$ odd about the magnetic field minimum. This specialization is an important one, for, although the mathematical formalism is applicable to $\tilde{\varphi}_m(z)$ odd or even, we find that the choice $\tilde{\varphi}_m(z)$ odd results in a mode with distinctly different properties from one with $\tilde{\varphi}_m(z)$ even.

We will examine the case in which $T_e \gg T_i$; $\omega \gg \Omega_i$; $\omega \gg (\pi/L)(T_i/m_i)^{1/2}$. For these frequencies the ion bounce motion is unimportant, and the ions are effectively unmagnetized; thus, the ion motion may be treated as an inertial response to the fluctuating electric field. Using the equation of motion, $m_i d\vec{v}_i/dt=-e\nabla\tilde{\Phi}$, the continuity equation, $\partial n_i/\partial t+\nabla\cdot(n_i\vec{v}_i)=0$, and $\nabla^2\tilde{\Phi}\simeq-(m^2/r^2)\tilde{\Phi}$, we obtain for the perturbed ion density

$$\tilde{n}_i=(en_i/m_i\omega^2)(m^2/r^2)\tilde{\varphi}_m. \tag{3}$$

We compute $\tilde{n}_e$ in the standard manner by integrating the linearized Vlasov equation along the unperturbed particle orbits. We consider the frequency range

$$\nu_{\rm eff}<\omega_{De}\ll\omega\lesssim\langle\omega_{be}\rangle\sim\omega_{*e}\ll\Omega_e, \tag{4}$$

where $\nu_{\rm eff}$ is the effective collision frequency for detrapping collisions; ω_{De} is the magnetic drift frequency; $\langle\omega_{be}\rangle$ is the average bounce frequency; ω_{*e} is the diamagnetic drift frequency; and Ω_e is the cyclotron frequency. We take the unperturbed distribution function to be locally Maxwellian, $f_{0e}=n_e(r)[2\pi T_e(r)/m_e]^{-3/2}\exp[-E/T_e(r)]$. With these assumptions, and neglecting finite-Larmor-radius effects, we follow Horton, Callen,

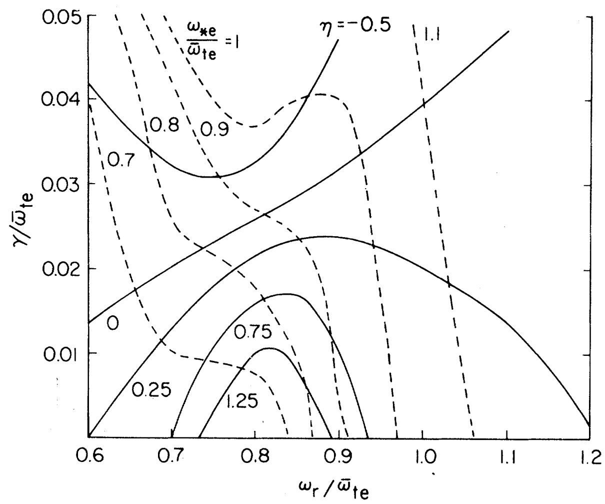

FIG. 1. Numerical solutions for growth rate γ, versus real frequency ω_r, for fixed η (solid curves) and fixed ω_{*e} (dashed curves) with $\epsilon=0.15$. $B_z=B_0[1-\epsilon\times\cos(2\pi z/L)]$; $\eta=d\ln T_e/d\ln n_e$; $\omega_{*e}=-(m/r)(T_e/eBn_e)\times dn_e/dr$. All frequencies are normalized to $\bar{\omega}_{te}$, where $\bar{\omega}_{te}\equiv(\pi/L)(2T_e/m_e)^{1/2}$. These results are for an argon plasma with $T_e=10$ eV; $n_e=5\times10^{10}/\text{cm}^3$; $n_e^{-1}dn_e/dr=2\ \text{cm}^{-1}$.

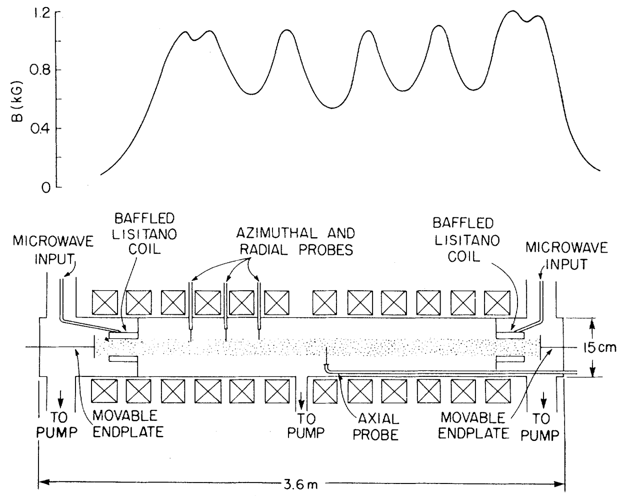

FIG. 2. Schematic diagram of the experimental device with the periodic magnetic field shown for $\epsilon=0.25$.

and Rosenbluth[4] to obtain

$$\tilde{n}_e=\frac{en_e}{T_e}[\tilde{\varphi}_m-n_e^{-1}\int d^3v\,f_{0e}(\omega-\omega_{*e}{}^T)I(t)], \qquad (5)$$

where

$$I(t)=i\int_{-\infty}^{t}dt'\,\tilde{\varphi}_m\exp[-\omega(t'-t)],$$

$$\omega_{*e}{}^T=[1+\eta(E/T_e-\tfrac{3}{2})]\omega_{*e},$$

$$\omega_{*e}=-\frac{m}{r}\frac{T_e}{eBn_e}\frac{dn_e}{dr},$$

$$\eta=d\ln T_e/d\ln n_e.$$

The time integral may be done formally by expanding $\tilde{\varphi}_m(z)$ in terms of bounce-frequency harmonics for trapped particles and transit-frequency harmonics for circulating particles. Performing this expansion one obtains resonant terms of the form $1/(\omega-p\omega_b)$, indicating that the mode is driven by particles whose bounce frequency equals the wave frequency. One continues by substituting the perturbed densities in Poisson's equation, $-\epsilon_0\nabla^2\Phi=e(\tilde{n}_i-\tilde{n}_e)$, and operating with $\int_{-L/2}^{L/2}dz\,\tilde{\varphi}_m{}^*/B_z$ to get a quadratic form. The resulting equation does not have any simple analytic form except in the rather uninteresting case $\omega\ll\langle\omega_{be}\rangle$ and will not be reproduced here.

The equation has been solved numerically, however, and we present the basic results in Fig. 1, where the growth rate, γ, is plotted versus the real frequency, ω_r, for various values of η and ω_{*e}. We see from these curves that for the normal case $\eta>0$ there is a region of unstable frequencies centered at a frequency slightly greater than $\langle\omega_{be}\rangle$, where $\langle\omega_{be}\rangle\simeq(2\epsilon)^{1/2}\bar{\omega}_{te}$. The maximum growth rate is $\gamma\sim0.03\bar{\omega}_{te}$ and occurs for $\eta\simeq0$. The curves for fixed ω_{*e} disclose that the modes with largest growth rate will occur for $\omega\simeq\omega_{*e}$. Since we have not solved for the radial eigenmode, the matching of the two sets of curves in Fig. 1 determines the radial location of the instability; but for the parameters of Fig. 1 (chosen to approximate our experimental conditions) the high mode number implied by $\omega\simeq\omega_{*e}$ vitiates the matching criterion: For almost any value of η one can find a mode number that allows $\omega\simeq\omega_{*e}$. Thus, we expect the frequency and radial location of the modes to be primarily determined by the η family of curves. Note also that these curves were generated by assuming $\tilde{\varphi}_m(z)=\sin(2\pi z/L)$. Since in a sinusoidal well the bounce frequency decreases as the turning point moves closer to $B_{\max}$, we expect that $\tilde{\varphi}_m(z)$ peaked nearer $B_{\max}$ would result in the instability range moving to lower frequency. This expectation is confirmed by numerical calculations.

To determine the mode dependence on trapping-well depth we have recomputed the curves of Fig. 1 for different values of ϵ. We find that the curves always retain the same basic shape, but that as ϵ increases, the curves shift outward to higher frequencies and upward to larger growth rates. The frequency band remains centered at $\omega\simeq(2\epsilon)^{1/2}\bar{\omega}_{te}$ or slightly greater. The largest

TABLE I. Theoretical predictions for the trapped-electron-scattering mode in cylindrical geometry.

Frequency	$\omega \simeq \omega_{*e} \simeq \langle\omega_{be}\rangle$
Dependence on collision frequency	mode exists only for $\nu_{\mathrm{eff}} < \omega$
Azimuthal variation	propagates with electron diamagnetic drift velocity $v_\theta \simeq r\omega_{*e}/m$
Radial variation	standing wave localized about $\eta \simeq 0$
Axial variation	standing wave $\tilde{\varphi}_m(z)$ odd about B_{min}
Dependence on trapping well	$\omega_r \propto \sqrt{\epsilon}$; γ increases with increasing ϵ

growth rate is always for $\eta \simeq 0$, although the upward shifting of the curves for higher ϵ results in instability for higher values of η as well. To facilitate comparison with the experimental results we summarize the basic theoretical predictions in Table I.

The experimental device is illustrated in Fig. 2. In uniform-field operation twelve magnets produce a field of about 1 kG flat to within ~5%. To produce four concatenate trapping wells four magnets are independently controlled to create a field which can be reasonably approximated by $B_z = B_0[1-\epsilon\cos(2\pi z/L)]$, where $L = 0.5$ m and ϵ may be varied from 0 to 0.4. The plasma is an rf-discharge, argon plasma produced by a Lisitano coil driven by ~25 W of microwave power at 3 GHz. The plasma formed typically has $n \sim 10^{10}-10^{11}/\mathrm{cm}^3$, $T_e \sim 5-10$ eV, $T_i \sim 0.2$ eV, and $n^{-1}dn/dr \sim 1-2\ \mathrm{cm}^{-1}$. For the electrons $\nu_{\mathrm{eff}} \simeq \nu_{en}/\epsilon$, where ν_{en} is the electron-neutral collision frequency; the neutral pressure may be varied such that the electrons are either collisional or collisionless with respect to bounce orbits.

For sufficiently low collision frequency we have observed a dramatic change in the plasma noise spectrum upon the application of a trapping magnetic field. The situation is illustrated in Fig. 3, where we have plotted the frequency spectrum with and without trapping field. The upper curve is for a trapping field with $\epsilon = 0.2$, $\langle\omega_{be}\rangle \simeq 1$ MHz; the lower curve is for uniform field. We observe that for the trapping-well case there is a tenfold increase in the noise level at frequencies near $\langle\omega_{be}\rangle$ and that there appears a coherent mode at a frequency somewhat below $\langle\omega_{be}\rangle$. The results are similar for all trapping-well depths above $\epsilon \simeq 0.1$: We typically see one or more modes excited, with the primary mode at a frequency somewhat below $\langle\omega_{be}\rangle$. The oscillations require low collision frequency; they disappear as ν_{eff} approaches ω.

The amplitude of the observed oscillations is small: Typically, $e\tilde{\varphi}/T_e \sim 0.01-0.1\%$; $\tilde{n}/n \sim 0.1\%$. These relatively low-level fluctuations are to be expected, since the predicted growth rates are small; and, as we shall describe below, the oscillations are highly localized, high-mode-number waves, which should make them susceptible to nonlinear saturation at relatively small amplitudes. The low-level saturated amplitudes imply that, at least for our cylindrical device, this particular mode may not have especially serious consequences for particle containment or energy loss; but, since the exact saturation mechanism is unknown, one must exercise caution in attempting to extend this result to toroidal devices.

We have examined in detail the coherent modes excited in the trapped-particle regime to determine their spatial characteristics. By cross-correlating the signals from two azimuthally separated probes we have been able to determine the azimuthal propagation velocity and the azimuthal wave number. We find that the waves propagate in the electron diamagnetic drift direction with velocity approximately equal to the diamagnetic drift velocity, $v_\theta \simeq r\omega_{*e}/m$. The observed mode

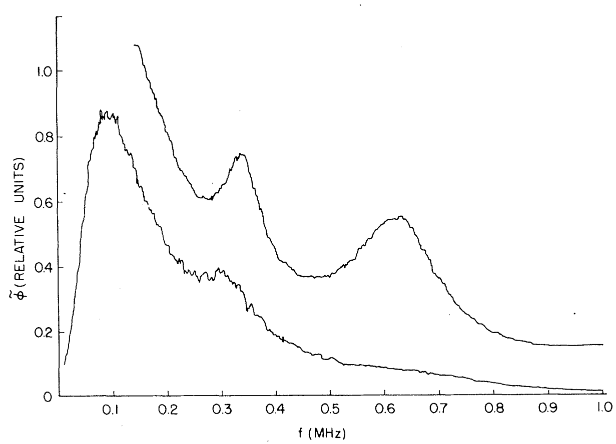

FIG. 3. Potential fluctuation spectrum at low collision frequency. Upper curve: trapping-well case with $\epsilon = 0.2$. Lower curve: uniform field. The peak at 90 kHz is instrumental.

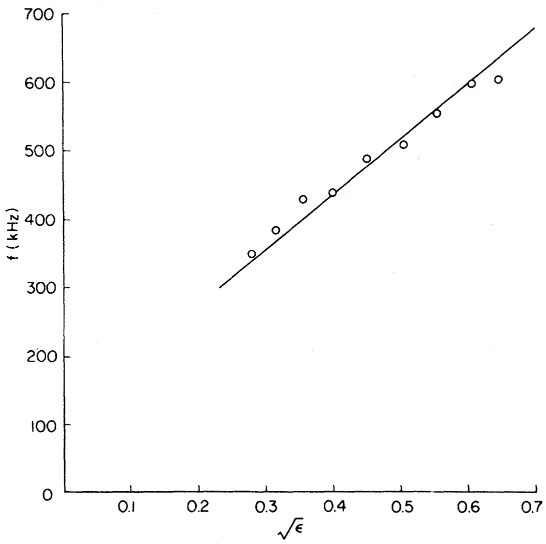

FIG. 4. Frequency of largest-amplitude trapped-electron wave versus $\sqrt{\epsilon}$.

numbers are high: Typically we have measured $m \sim 6-12$. We have measured the fluctuation amplitude, $\tilde{\varphi}_{\mathrm{rms}}$, as a function of both radial and axial position. We find that the oscillations are strongly localized radially, with the peak amplitude occurring in the region of minimum η in agreement with theoretical predictions. In the axial direction we observe that $\tilde{\varphi}_{\mathrm{rms}}(z)$ is periodic along z in a manner consistent with the assumption that $\tilde{\varphi}_m(z)$ is odd about B_{min}. To confirm the fact that $\tilde{\varphi}_m(z)$ is indeed an odd function, we have taken cross-correlation measurements between probes at fixed axial positions but carefully aligned on the same magnetic field line. These results are also consistent with $\tilde{\varphi}_m(z)$ odd about B_{min}.

We have investigated the mode dependence on ϵ, the trapping-well depth. In Fig. 4 we have plotted the frequency of the primary mode versus $\sqrt{\epsilon}$. We observe that the frequency increases linearly with $\sqrt{\epsilon}$ as predicted by the theory, although the relation is not simply $\omega \propto \sqrt{\epsilon}$, since the curve does not have a zero frequency intercept. The saturated-wave amplitude also exhibits an increase with increasing $\sqrt{\epsilon}$; we observe that $\tilde{\varphi}_{\mathrm{rms}}$ increases somewhat faster than linearly with $\sqrt{\epsilon}$.

In summary, we have observed new oscillations in a linear device in the presence of a spatially periodic magnetic field. A comparison of the experimental observations with the theoretical predictions summarized in Table I shows that the observed waves are consistent with the theoretical predictions in virtually all respects. We therefore identify the oscillations as belonging to the trapped-electron-scattering mode.

We thank G. Rewoldt for helpful discussions and for development of the computer code used in the numerical solutions.

*Work supported by the National Science Foundation under Grant No. GK-37979-*X*.

[1]There have been many papers written on the subject of trapped-particle modes. Probably the best published review paper is B. B. Kadomtsev and O. P. Pogutse, Nucl. Fusion 11, 67 (1971).

[2]B. Coppi and G. Rewoldt, Massachusetts Institute of Technology, Research Laboratory of Electronics, Report No. PRR-749, 1974 (to be published).

[3]B. Coppi, Phys. Rev. Lett. 29, 1076 (1972).

[4]C. W. Horton, Jr., J. D. Callen, and M. N. Rosenbluth, Phys. Fluids 14, 2019 (1971).

Calculated Energy Levels and Optical Absorption in *n*-Type Si Accumulation Layers at Low Temperature

Frank Stern
IBM Thomas J. Watson Research Center, Yorktown Heights, New York 10598

(Received 9 July 1974)

Self-consistent sub-band splittings and inter-sub-band optical matrix elements are calculated for *n*-type accumulation layers at temperatures low enough that the bulk carriers are frozen out. The energy splittings are sensitive to the concentration of *acceptor* impurities in the surface space-charge layer.

Quantum effects in accumulation layers have been studied theoretically by several authors,[1-3] and experimental results have been obtained for InAs,[4] Te,[5,6] PbTe,[7] and Si.[8] This paper gives results of numerical self-consistent calculations for sub-band splittings of accumulation layers in